

## Combined optical sizing and acoustical characterization of single freely-floating microbubbles

Luan, Ying; Renaud, Guillaume; Raymond, Jason L.; Segers, Tim; Lajoinie, Guillaume; Beurskens, Robert; Mastik, Frits; Kokhuis, Tom J A; Van Der Steen, Antonius F W; Versluis, Michel

**DOI**

[10.1063/1.4971391](https://doi.org/10.1063/1.4971391)

**Publication date**

2016

**Document Version**

Final published version

**Published in**

Applied Physics Letters

**Citation (APA)**

Luan, Y., Renaud, G., Raymond, J. L., Segers, T., Lajoinie, G., Beurskens, R., Mastik, F., Kokhuis, T. J. A., Van Der Steen, A. F. W., Versluis, M., & De Jong, N. (2016). Combined optical sizing and acoustical characterization of single freely-floating microbubbles. *Applied Physics Letters*, *109*(23), Article 234104. <https://doi.org/10.1063/1.4971391>

**Important note**

To cite this publication, please use the final published version (if applicable).  
Please check the document version above.

**Copyright**

Other than for strictly personal use, it is not permitted to download, forward or distribute the text or part of it, without the consent of the author(s) and/or copyright holder(s), unless the work is under an open content license such as Creative Commons.

**Takedown policy**

Please contact us and provide details if you believe this document breaches copyrights.  
We will remove access to the work immediately and investigate your claim.

## Combined optical sizing and acoustical characterization of single freely-floating microbubbles

Ying Luan, Guillaume Renaud, Jason L. Raymond, Tim Segers, Guillaume Lajoie, Robert Beurskens, Frits Mastik, Tom J. A. Kokhuis, Antonius F. W. van der Steen, Michel Versluis, and Nico de Jong

Citation: *Appl. Phys. Lett.* **109**, 234104 (2016); doi: 10.1063/1.4971391

View online: <http://dx.doi.org/10.1063/1.4971391>

View Table of Contents: <http://aip.scitation.org/toc/apl/109/23>

Published by the [American Institute of Physics](#)

---

### Articles you may be interested in

[Decreasing luminescence lifetime of evaporating phosphorescent droplets](#)

*Appl. Phys. Lett.* **109**, 234103234103 (2016); 10.1063/1.4971987

[Universality in freezing of an asymmetric drop](#)

*Appl. Phys. Lett.* **109**, 234105234105 (2016); 10.1063/1.4971995

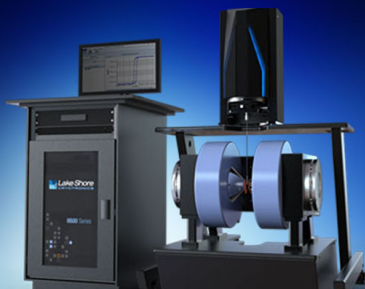
[Vaporization and recondensation dynamics of indocyanine green-loaded perfluoropentane droplets irradiated by a short pulse laser](#)

*Appl. Phys. Lett.* **109**, 243701243701 (2016); 10.1063/1.4972184

[Reconfigurable heat-induced spin wave lenses](#)


*Appl. Phys. Lett.* **109**, 232407232407 (2016); 10.1063/1.4971829

---



**NEW 8600 Series VSM**

For fast, highly sensitive  
measurement performance

LEARN MORE 

## Combined optical sizing and acoustical characterization of single freely-floating microbubbles

Ying Luan,<sup>1</sup> Guillaume Renaud,<sup>1,2</sup> Jason L. Raymond,<sup>1</sup> Tim Segers,<sup>3</sup> Guillaume Lajoinie,<sup>3</sup> Robert Beurskens,<sup>1</sup> Frits Mastik,<sup>1</sup> Tom J. A. Kokhuis,<sup>1</sup> Antonius F. W. van der Steen,<sup>1,4</sup> Michel Versluis,<sup>3</sup> and Nico de Jong<sup>1,4</sup>

<sup>1</sup>Biomedical Engineering Thoraxcenter, Erasmus Medical Center, 3015 CN Rotterdam, The Netherlands

<sup>2</sup>Sorbonne Universités, UPMC Univ Paris 06, CNRS UMR 7371, INSERM UMR S 1146,

Laboratoire d'Imagerie Biomédicale, Paris, France

<sup>3</sup>Physics of Fluids group and MIRA Institute for Biomedical Technology and Technical Medicine, University of Twente, 7522 NB Enschede, The Netherlands

<sup>4</sup>Acoustical Wavefield Imaging, Delft University of Technology, 2628 CD Delft, The Netherlands

(Received 13 August 2016; accepted 21 November 2016; published online 7 December 2016)

In this study we present a combined optical sizing and acoustical characterization technique for the study of the dynamics of single freely-floating ultrasound contrast agent microbubbles exposed to long burst ultrasound excitations up to the milliseconds range. A co-axial flow device was used to position individual microbubbles on a streamline within the confocal region of three ultrasound transducers and a high-resolution microscope objective. Bright-field images of microbubbles passing through the confocal region were captured using a high-speed camera synchronized to the acoustical data acquisition to assess the microbubble response to a 1-MHz ultrasound burst. Nonlinear bubble vibrations were identified at a driving pressure as low as 50 kPa. The results demonstrate good agreement with numerical simulations based on the shell-buckling model proposed by Marmottant *et al.* [J. Acoust. Soc. Am. **118**, 3499–3505 (2005)]. The system demonstrates the potential for a high-throughput *in vitro* characterization of individual microbubbles. Published by AIP Publishing. [<http://dx.doi.org/10.1063/1.4971391>]

Lipid-coated microbubbles are widely used as ultrasound contrast agents (UCA) for medical ultrasound imaging.<sup>1</sup> Their use has also been investigated extensively for targeted molecular imaging and therapeutic applications, e.g., for local drug-delivery and sonothrombolysis.<sup>2,3</sup> The nonlinear radial dynamic response of single microbubbles exposed to ultrasound, especially to long burst excitations, are of great interest for developing imaging and drug delivery strategies.<sup>4–6</sup> Previous studies using acoustical or optical techniques to determine the microbubble response to ultrasound excitation, have demonstrated a myriad of nonlinear behaviors specific to lipid-coated microbubbles. These behaviors include asymmetric oscillation due to buckling and rupture of the lipid shell,<sup>7</sup> subharmonic emission,<sup>8</sup> and compression-only behavior.<sup>9</sup> The precedence of these behaviors is influenced by both the microbubble size with respect to the ultrasonic driving frequency (e.g., resonance effects) and the lipid shell properties. Therefore, practical microbubble characterization techniques should incorporate measurement of the radial dynamic response simultaneously with accurate sizing of single isolated bubbles.<sup>10</sup>

Conventional single microbubble characterization techniques are generally restricted by limitations of the sensitivity or temporal resolution of the applied method. For example, acoustical methods offer excellent temporal resolution but require an accurate calibration of the system and a high sensitivity to detect echo signals scattered from a single bubble.<sup>12</sup> Optical methods have been employed using (ultra) high-speed cameras to capture the instantaneous microbubble vibrations.<sup>13,14</sup> However, the frame rate is generally less than 25 Mfps,<sup>5,6,8</sup> and the recording time is restricted by the frame

rate and the number of recorded frames unless complex timing schemes are used.<sup>15</sup> Techniques in which isolated microbubbles are manipulated or confined within a capillary or a flow channel can overcome these limitations to some degree.<sup>10,11</sup> However, the confinement may hinder free motion of the microbubbles<sup>16</sup> and may influence the driving acoustic field and the reradiated pressure levels.

The objective of the present letter is to introduce a technique that provides quantitative characterization of the vibrational response of single freely-floating microbubbles exposed to long low-amplitude ultrasound bursts. A previously introduced acoustical characterization system based on the measurement of the scattering signal from individual particles in the geometrical scattering regime was utilized in this study.<sup>17–19</sup> Briefly, a pair of transmit/receive high-frequency (HF, 30 MHz) focused transducers and a low-frequency (LF, 1 MHz) focused transducer were confocally aligned in a water tank (25 mL volume) as shown in Figure 1(a). The role of the HF transducers was to measure the relative change of the bubble radius produced by the LF excitation, as described previously.<sup>17,20</sup> Because the scattered acoustic signal (HF response) is directly proportional to relative amplitude modulation (LF response) for bubbles with the radius above 1  $\mu\text{m}$ , an absolute calibration for this method is not necessary. The setup is allowed for the measurement of single microbubbles from a diluted suspension in free flow, and the measurement time duration is limited only by the size of the effective focal region and the velocity of the microbubble in the confocal measurement volume, normally in the milliseconds range. The major limitation of this system, however, is that the absolute size of individual microbubbles cannot be determined due

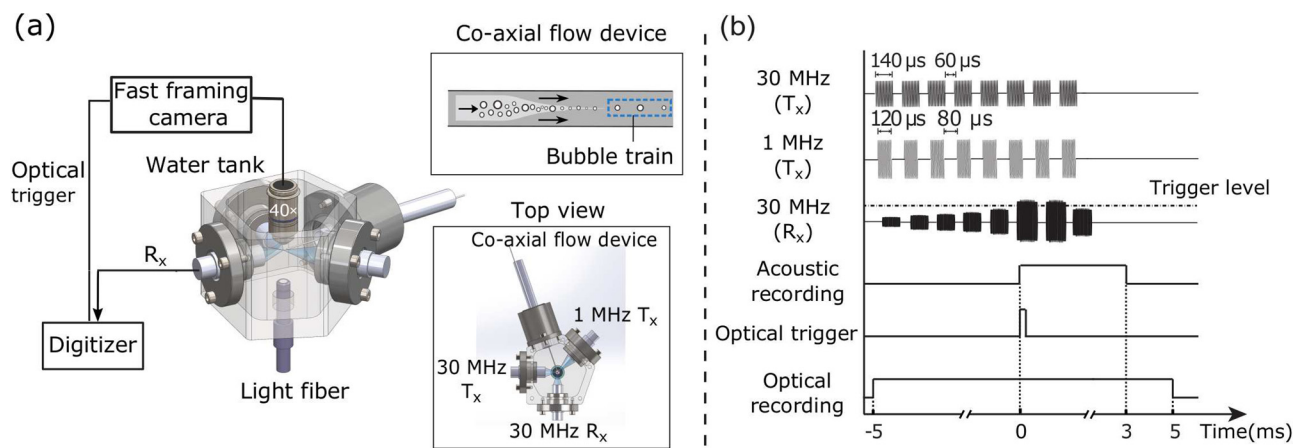


FIG. 1. (a) A schematic plot of the experimental setup. Subplots show the co-axial flow device for the generation of a bubble train (with a spacing of  $\sim 300 \mu\text{m}$  between two bubbles) and the top-view of the water tank configured with a co-axial flow device, a pair of transmitting transducers (low-frequency (LF) 1 MHz, high-frequency (HF) 30 MHz,  $T_x$ ) and a receiving transducer (HF 30 MHz,  $R_x$ ); (b) The timing diagram of a recording.

to the fact that the exact location of the bubble with respect to the probing transducer position is unknown.<sup>19–21</sup> In this study, we aim to develop a combined optical sizing and acoustical characterization technique using a coaxial-flow device to isolate individual microbubbles to form a bubble train which can be directed to the confocal region of the ultrasound transducer and a high-resolution microscope objective. As such, an optical image of the bubble was captured while at the very same moment the acoustical response of the vibrating bubble was recorded.

In order to demonstrate the feasibility of this idea, an experimental setup with simultaneous optical sizing and acoustical measurement functions was developed. A coaxial-flow device (developed in house) was mounted on a gimbal mount and coupled to the water tank, as illustrated by Figure 1(a). It consisted of an inner flow containing the bubble suspension confined by a  $150 \mu\text{m}$  fused silica capillary. A fine tip of the capillary was produced by pulling it after melting in a flame which resulted in an outlet diameter of  $10 \mu\text{m}$ . The outlet was located co-axially within the center of a blunt tip dispensing needle ( $1.5 \text{ mm}$  diameter) containing the co-axial sheath flow. At the exit of the glass capillary, the bubble flow was accelerated by the sheath flow such that the microbubbles were separated from each other to form a bubble train,<sup>22</sup> as shown in Figure 1(a). The inner flow ( $\sim 2.5 \text{ mm/s}$ ) and the co-axial sheath flow ( $\sim 100 \text{ mm/s}$ ) were driven by separate syringe pumps to control the approximate spacing between individual bubbles ( $\sim 300 \mu\text{m}$  typical). This allowed a single microbubble (after exiting the co-axial flow device) to pass at a time through the confocal volume of the three ultrasound beams. A microscope with a  $40\times$  water-immersion objective (numerical aperture (NA) = 0.8; Olympus, Zoeterwoude, the Netherlands) and a CMOS-based high-speed camera (Photron APX-RS; Photron Ltd., West Wycombe, UK) were positioned above the water tank to image the co-axial flow from above. An optical light guide (SCHOTT AG, Mainz, Germany) mounted at the bottom of the water tank was connected to a halogen light source (KL1500LCD, Schott, Germany) to illuminate the region-of-interest, see Figure 1(a).

The optical field of view was aligned with the acoustical focus prior to the experiment. Briefly, a thin needle ( $300 \mu\text{m}$

diameter) with the same length as the body length of the  $40\times$  objective plus its working distance ( $3.3 \text{ mm}$ ) was manipulated using the x-y stage until a maximum echo signal from the 30 MHz probes was found. Then the co-axial flow device was manipulated in three dimensions to direct the bubble train to the aligned confocal region. As the bubbles traversed through the focal region the received echo varied in amplitude, as shown by Figure 1(b). When the echo was above the threshold amplitude (10% of the vertical range of the digitizer), the acoustic response of a microbubble was digitized and recorded (PX14400, Signatec, CA, USA). Simultaneously, a trigger signal was sent to the high-speed camera running at 6000 frames per second (fps) with an exposure time of  $50 \mu\text{s}$  to capture bright-field images of the very same microbubble presented in the optical field of view. The camera was operated to capture 60 frames for a 10 ms time duration, with 5 ms before and 5 ms after the optical trigger signal had arrived, see Figure 1(b).

We plotted the location of 51 single microbubbles captured when the optical recording was triggered. For a well-aligned system, the positions of bubbles in the trigger frame should be grouped within a small region defined by the acoustical focus. Figure 2 shows a typical image frame of a microbubble passing through the focal plane, and a superposition of the bubble location of 50 other recordings at the trigger frame (indicated by open circle symbols). The histogram of microbubble locations grouped into  $25 \mu\text{m}$  bins along X and Y dimensions of the image frame, respectively, were plotted. The statistical distribution of microbubbles were estimated by fitting the histograms with a Gaussian function. The maximum integral over a range of  $150 \mu\text{m}$  along each dimension (99.5% along X dimension, and 98.8% along Y dimension) was found, resulting in an overlapping area of  $150 \mu\text{m} \times 150 \mu\text{m}$ . This is around the projected area of the acoustic focal volume based on the characteristics of the HF transducer. The optical recording shows that 49 out of 51 ( $\sim 96\%$ ) bubbles were distributed within this region at the trigger frame, which demonstrates that each microbubble captured optically was also measured acoustically.

Phospholipid-coated microbubbles with a perfluorobutane ( $\text{C}_4\text{F}_{10}$ ) gas core were made by sonication.<sup>23</sup> The vibrational

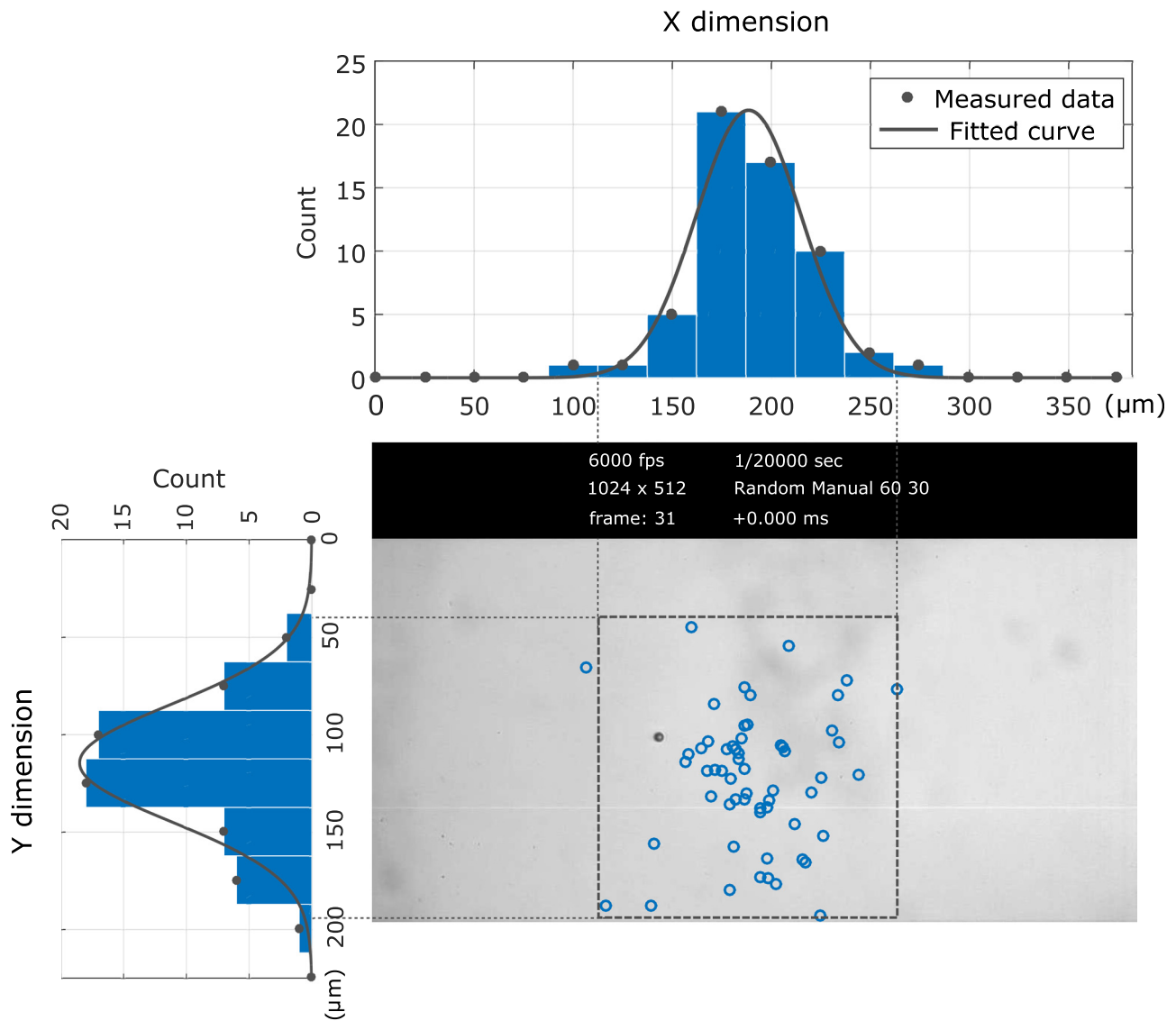


FIG. 2. An in-focus video frame of a microbubble passing through the focal plane in the optical field of view and the location of 50 other microbubbles (circles) when the trigger signal was sent to the camera. The histogram was plotted and was fitted with a Gaussian function along both X and Y dimensions. The estimated acoustical focal region of  $150 \times 150 \mu\text{m}$  was plotted (the dashed rectangle).

response (radius-time curve) of a total of 72 single microbubbles to a 1 MHz ultrasound burst with a peak negative pressure of 50 kPa was measured and analyzed. The measured resting radius ( $R_{\text{meas}}$ ) of each microbubble was estimated from a selected in-focus image from an optical recording using an edge-tracking minimum cost algorithm.<sup>24</sup> This is a dynamic programming algorithm by first selecting a center point of a microbubble, which was then used to radially resample the bubble contour and its intensity profile until an optimal contour of the bubble was detected. The uncertainty of the optical size measurement combining the random and the systematic error was  $0.1 \mu\text{m}$  based on an evaluation following Ref. 11.

The received echo signal was first band-pass filtered around the interrogation frequency (bandwidth of 20–40 MHz). Then the envelope of the signal was calculated to yield the relative bubble oscillation amplitude  $\varepsilon(t) = \Delta R/R_0$  (where  $R_0$  is the initial bubble radius).<sup>18,19</sup> The frequency spectrum of  $\varepsilon(t)$  was then derived by applying a Fast Fourier Transform (FFT), from which the following parameters were obtained:  $\varepsilon_f$  is the relative oscillation amplitude at the fundamental frequency, i.e., the

driving frequency;  $\varepsilon_{2f}$  is the relative oscillation amplitude at the second harmonic frequency, i.e., at twice the driving frequency;  $(A_{\text{exp}} - A_{\text{com}}) \times 100\%$  (where  $A_{\text{exp}} = |R_{\text{max}} - R_0|/R_0$  and  $A_{\text{com}} = |R_{\text{min}} - R_0|/R_0$  are the relative amplitude of the expansion and the compression phase), to assess the asymmetry of the dynamic response.<sup>25</sup> To validate the experimental results, the nonlinear bubble dynamics model proposed by Marmottant *et al.*<sup>7</sup> was used to simulate the response of the lipid-coated microbubbles. For the simulation, we chose typical viscoelastic parameters from literature. The elastic state was selected as the initial state of the bubble, with an initial surface tension  $\sigma(R_0) = 0.02 \text{ N/m}$ . The elasticity was taken as  $\chi = 2.5 \text{ N/m}^{25}$  and the shell viscosity  $\kappa_s(R_0)$  was considered to be dependent on the initial bubble radius,<sup>22,26</sup> instead of being a constant as was defined in the Marmottant model

$$\kappa_s(R_0) = 10^{-9.0+0.28R_0} / (1 \text{ m}) \text{ kg/s.}$$

We observed nonlinear and asymmetric bubble responses to the 1-MHz ultrasound burst for single microbubbles with a resting radius ranging from  $1.5 \mu\text{m}$  to  $4.6 \mu\text{m}$ . A plot of the

relative oscillation amplitude at the fundamental frequency ( $\varepsilon_f$ ) and at the second harmonic ( $\varepsilon_{2f}$ ), as a function of the measured bubble radius ( $R_{\text{meas}}$ ) is shown in Figures 3(a) and 3(b). The maximum response ( $\varepsilon_f \approx 35\%$ ,  $\varepsilon_{2f} \approx 11\%$ ) can be found for microbubbles with a radius of  $\sim 3.4 \mu\text{m}$ , which is a typical resonant size for a driving frequency of 1 MHz, as reported previously.<sup>23,27</sup> The experimental data showed good agreement with the simulation results. Figures 3(c) and 3(d) illustrates the asymmetric vibrational response, indicated by the difference between the relative amplitude of the expansion and the compression phase ( $A_{\text{exp}} - A_{\text{com}}$ ), versus bubble size  $R_{\text{meas}}$ . Two typical examples of measured radius-time responses showing symmetric response (example 1, Figs. 3(d)-1) and compression-dominant vibrations (example 2, Fig. 3(d)-2) were plotted. Note that examples 1 and 2 refer to the same bubbles circled in Figure 3(c). Results indicate that  $\sim 80\%$  of the measured bubbles showed symmetrical oscillations at 50 kPa ( $-4\% < A_{\text{exp}} - A_{\text{com}} < 4\%$ ), while

20% of the bubbles showed compression-dominant vibrations ( $A_{\text{exp}} - A_{\text{com}} < -4\%$ ), as shown in Fig. 3(c). The latter bubbles predominantly (13 out of 15 bubbles) have a resting radius between  $3 \mu\text{m}$  and  $4 \mu\text{m}$ , and are therefore, close to their resonant size at a driving frequency of 1 MHz; compare with Fig. 3(a).

It was reported by previous studies that nonlinear and asymmetric bubble responses can occur at the low acoustic pressure regime (tens of kilopascals).<sup>25,27</sup> These phenomena were considered not only to be influenced by the resting bubble size, but also to be dependent on the initial surface tension due to the presence of the phospholipid coating,<sup>28,29</sup> which can greatly vary among individual bubbles.<sup>27,30</sup> This explains the variability in the asymmetric response among microbubbles within the same size range, see the two examples (and other bubbles) in Fig. 3(d) that nearly have the same size. The compression-dominated vibration can be due to the buckled lipid coating which cancels out the initial

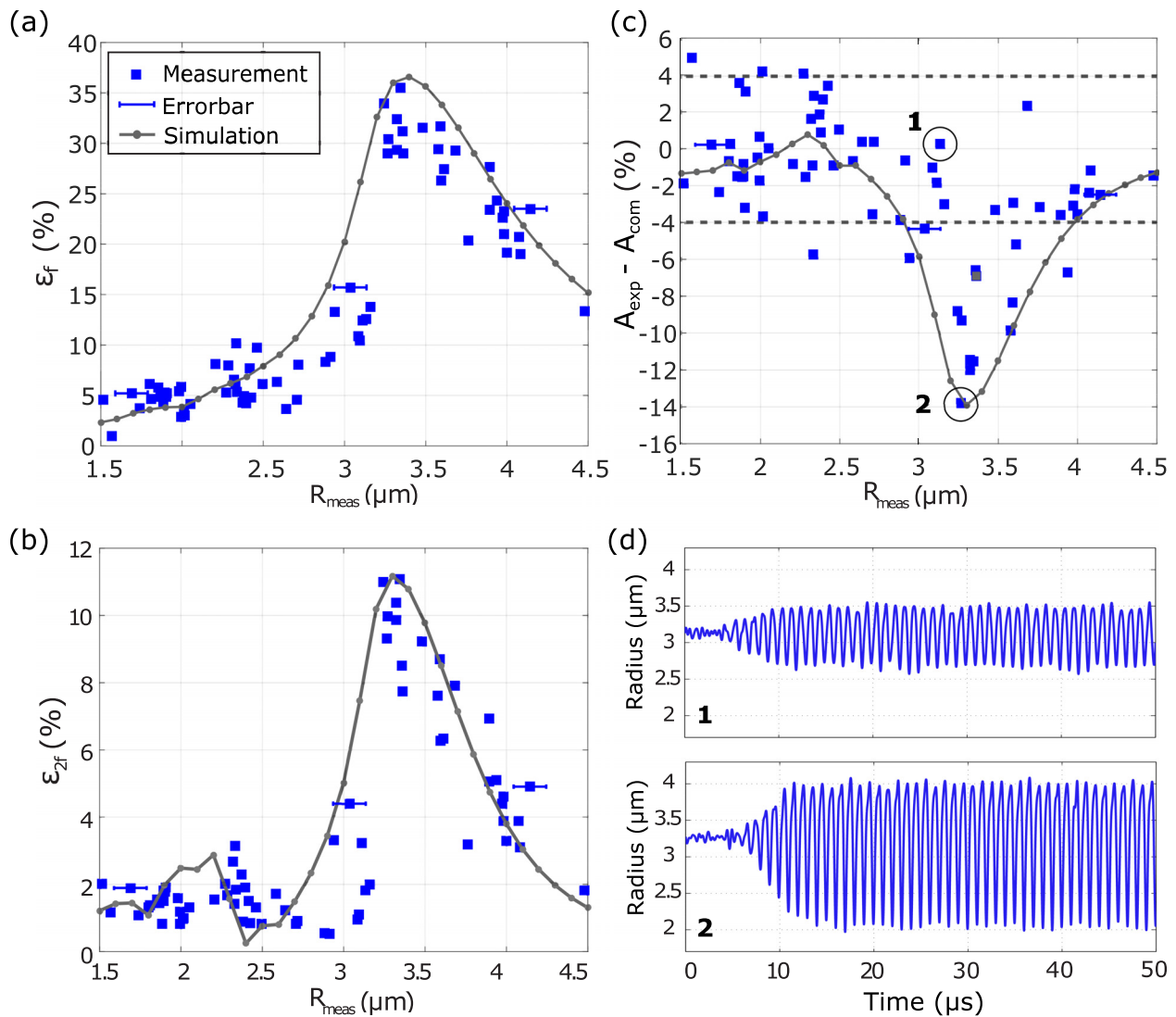


FIG. 3. (a) The measured and simulated relative oscillation amplitude at fundamental frequency and (b) at second harmonic frequency as a function of the measured microbubble size ( $R_{\text{meas}}$ ), at the applied pressure of 50 kPa. (c) The measured and simulated difference between the relative amplitude of the expansion and the compression phase, as a function of the measured bubble size ( $R_{\text{meas}}$ ), at a driving pressure of 50 kPa. (d) Examples of measured radius-time curves of two microbubbles during the first  $50 \mu\text{s}$  showing symmetrical vibrations (1) and compression-dominant vibrations (2), respectively. The error of size estimation ( $\pm 0.1 \mu\text{m}$ ) were plotted for three individual bubbles of different sizes.

surface tension, leading to elevated harmonic response.<sup>28</sup> An earlier study by Sijl *et al.*<sup>25</sup> suggested a maximum negative offset of the bubble radial dynamics (i.e., compression-only behavior) at the resonance frequency through a weakly nonlinear analysis of Marmottant model, which is in agreement with the observations in this study, as shown by Figs. 3(a)–3(c).

In conclusion, in this letter we have described a combined acoustical and optical measurement technique which was capable of acquiring radius-time responses of single freely-floating UCA microbubbles. The bubble responses under prolonged ultrasound exposure can be measured. This technique overcomes the limitations in the sampling rate and the exposure time of an ultra-high speed imaging system, and demonstrates great potential for high-throughput *in vitro* statistical characterization of UCA populations.

The authors would like to thank Michiel Manten and Geert Springeling from the Department of Experimental Medical Instrumentation, Erasmus MC for manufacturing the custom water bath. The valuable discussions with Dr. Hans Bosh at the Department of Biomedical Engineering, Erasmus MC are appreciated. This work was supported in part by NanoNextNL, a micro and nanotechnology consortium of the Government of the Netherlands and 130 partners.

- <sup>1</sup>J. R. Lindner, "Microbubbles in medical imaging: current applications and future directions," *Nat. Rev. Drug Discov.* **3**, 527–532 (2004).
- <sup>2</sup>R. Medel, R. W. Crowley, M. S. McKisic, A. S. Dumont, and N. F. Kassell, "Sonothrombolysis: An emerging modality for the management of stroke," *Neurosurgery* **65**, 979–993 (2009).
- <sup>3</sup>E. Stride and N. Saffari, "Microbubble ultrasound contrast agents: A review," *Proc. Inst. Mech. Eng., H* **217**, 429–447 (2003).
- <sup>4</sup>B. A. Schrope and V. L. Newhouse, "Second harmonic ultrasonic blood perfusion measurement," *Ultrasound Med. Biol.* **19**, 567–579 (1993).
- <sup>5</sup>E. C. Gelderblom, H. J. Vos, F. Mastik, T. Faez, Y. Luan, T. J. A. Kokhuis, A. F. W. van der Steen, D. Lohse, N. de Jong, and M. Versluis, "Brandaris 128 ultra-high-speed imaging facility: 10 years of operation, updates, and enhanced features," *Rev. Sci. Instrum.* **83**, 103706 (2012).
- <sup>6</sup>Y. Luan, G. Lajoinie, E. C. Gelderblom, I. Skachkov, A. F. W. van der Steen, H. J. Vos, M. Versluis, and N. de Jong, "Lipid shedding from single oscillating microbubbles," *Ultrasound Med. Biol.* **40**, 1834–1846 (2014).
- <sup>7</sup>P. Marmottant, S. van der Meer, M. Emmer, M. Versluis, N. de Jong, S. Hilgenfeldt, and D. Lohse, "A model for large amplitude oscillations of coated bubbles accounting for buckling and rupture," *J. Acoust. Soc. Am.* **118**, 3499–3505 (2005).
- <sup>8</sup>T. Faez, M. Emmer, M. Docter, J. Sijl, M. Versluis, and N. de Jong, "Characterizing the subharmonic response of phospholipid-coated microbubbles for carotid imaging," *Ultrasound Med. Biol.* **37**, 958–970 (2011).
- <sup>9</sup>N. de Jong, M. Emmer, C. T. Chin, A. Bouakaz, F. Mastik, D. Lohse, and M. Versluis, "'Compression-only' behavior of phospholipid-coated contrast bubbles," *Ultrasound Med. Biol.* **33**, 653–656 (2007).
- <sup>10</sup>J. Sijl, H. J. Vos, T. Rozendal, N. de Jong, D. Lohse, and M. Versluis, "Combined optical and acoustical detection of single microbubble dynamics," *J. Acoust. Soc. Am.* **130**, 3271–3281 (2011).

- <sup>11</sup>D. Maresca, M. Emmer, P. L. M. J. van Neer, H. J. Vos, M. Versluis, M. Muller, N. de Jong, and A. F. W. van der Steen, "Acoustic sizing of an ultrasound contrast agent," *Ultrasound Med. Biol.* **36**, 1713–1721 (2010).
- <sup>12</sup>J. Sijl, E. Gaud, P. J. Frinking, M. Arditi, N. de Jong, D. Lohse, and M. Versluis, "Acoustic characterization of single ultrasound contrast agent microbubbles," *J. Acoust. Soc. Am.* **124**, 4091–4097 (2008).
- <sup>13</sup>P. A. Dayton, J. S. Allen, and K. W. Ferrara, "The magnitude of radiation force on ultrasound contrast agents," *J. Acoust. Soc. Am.* **112**, 2183–2192 (2002).
- <sup>14</sup>A. Bouakaz, M. Versluis, and N. de Jong, "High-speed optical observations of contrast agent destruction," *Ultrasound Med. Biol.* **31**, 391–399 (2005).
- <sup>15</sup>T. J. A. Kokhuis, Y. Luan, F. Mastik, R. H. S. H. Beurskens, M. Versluis, and N. de Jong, "Segmented high speed imaging of vibrating microbubbles during long ultrasound pulses," in 2012 IEEE International Ultrasonics Symposium (IUS) (2012).
- <sup>16</sup>V. Garbin, D. Cojoc, E. Ferrari, E. Di Fabrizio, M. L. J. Overvelde, M. Versluis, S. M. van der Meer, N. de Jong, and D. Lohse, "Time-resolved nanoseconds dynamics of ultrasound contrast agent microbubbles manipulated and controlled by optical tweezers," *Proc. SPIE* **6326**, 63261V (2006).
- <sup>17</sup>G. Renaud, J. G. Bosch, A. F. W. van der Steen, and N. de Jong, "An 'acoustical camera' for *in vitro* characterization of contrast agent microbubble vibrations," *Appl. Phys. Lett.* **100**, 101911 (2012).
- <sup>18</sup>G. Renaud, J. G. Bosch, A. F. W. van der Steen, and N. de Jong, "Chirp resonance spectroscopy of single lipid-coated microbubbles using an 'acoustical camera'," *J. Acoust. Soc. Am.* **132**, EL470-5 (2012).
- <sup>19</sup>G. Renaud, J. G. Bosch, A. F. W. van der Steen, and N. de Jong, "Low-amplitude non-linear volume vibrations of single microbubbles measured with an 'Acoustical Camera'," *Ultrasound Med. Biol.* **40**, 1282–1295 (2014).
- <sup>20</sup>R. A. Roy and R. E. Apfel, "Mechanical characterization of microparticles by scattered ultrasound," *J. Acoust. Soc. Am.* **87**, 2332–2341 (1990).
- <sup>21</sup>C. E. Everbach, D. B. Khismatullin, J. T. Flaherty, and R. A. Roy, "Characterization of individual submicron perfluorocarbon gas bubbles by ultrasonic backscatter," *Acoust. Res. Lett.* **6**, 175–181 (2005).
- <sup>22</sup>T. Segers and M. Versluis, "Acoustic bubble sorting for ultrasound contrast agent enrichment," *Lab Chip* **14**, 1705–1714 (2014).
- <sup>23</sup>A. L. Klibanov, P. T. Rasche, M. S. Hughes, J. K. Wojdyla, K. P. Galen, J. H. Wible, Jr., and G. H. Brandenburger, "Detection of individual microbubbles of ultrasound contrast agents: Imaging of free-floating and targeted bubbles," *Invest. Radiol.* **39**, 187–195 (2004).
- <sup>24</sup>S. M. van der Meer, B. Dollet, M. M. Voormolen, C. T. Chien, A. Bouakaz, N. de Jong, M. Versluis, and D. Lohse, "Microbubble spectroscopy of ultrasound contrast agents," *J. Acoust. Soc. Am.* **121**, 648–656 (2007).
- <sup>25</sup>J. Sijl, M. Overvelde, B. Dollet, V. Garbin, N. de Jong, D. Lohse, and M. Versluis, "Compression-only" behavior: a second-order nonlinear response of ultrasound contrast agent microbubbles," *J. Acoust. Soc. Am.* **129**, 1729–1739 (2011).
- <sup>26</sup>M. Emmer, H. J. Vos, M. Versluis, and N. de Jong, "Radial modulation of single microbubbles," *IEEE Trans. Ultrason. Ferroelectr. Freq. Control* **56**, 2370–2379 (2009).
- <sup>27</sup>M. Overvelde, V. Garbin, J. Sijl, B. Dollet, N. de Jong, D. Lohse, and M. Versluis, "Nonlinear shell behavior of phospholipid-coated microbubbles," *Ultrasound Med. Biol.* **36**, 2080–2092 (2010).
- <sup>28</sup>N. de Jong, M. Emmer, A. van Wamel, and M. Versluis, "Ultrasonic characterization of ultrasound contrast agents," *Med. Biol. Eng. Comput.* **47**, 861–873 (2009).
- <sup>29</sup>M. Emmer, A. van Wamel, D. E. Goertz, and N. de Jong, "The onset of microbubble vibration," *Ultrasound Med. Biol.* **33**, 941–949 (2007).
- <sup>30</sup>D. E. Goertz, N. de Jong, and A. F. van der Steen, "Attenuation and size distribution measurements of definitly and manipulated definitly populations," *Ultrasound Med. Biol.* **33**, 1376–1388 (2007).